Journal of Materials Chemistry A

Chemically Inert Covalently Networked Triazole-based Solid Polymer Electrolytes for Stable All-solid-state Lithium Batteries

Journal:	*Journal of Materials Chemistry A*
Manuscript ID	TA-COM-06-2019-005885.R1
Article Type:	Communication
Date Submitted by the Author:	02-Aug-2019
Complete List of Authors:	Shi, Yi; Sun Yat-Sen University, School of Materials Science and Engineering Chen, Yang; Fudan University; University of Houston Liang, Yanliang; University of Houston Andrews, Justin; Texas A&M University, Department of Chemistry Dong, Hui; University of Houston, Electrical and Computer Engineering ; University of Houston Yuan, Mengying; University of Houston, Ding, Wenyue; University of Houston Banerjee, Sarbajit; Texas A&M University, Department of Chemistry Ardebili, Haleh; University of Houston, Department of Mechanical Engineering Robertson, Megan; University of Houston, Chemical and Biomolecular Engineering Cui, Xiaoli; Fudan University, Yao, Yan; University of Houston, Electrical and Computer Engineering

COMMUNICATION

Chemically Inert Covalently Networked Triazole-based Solid Polymer Electrolytes for Stable All-solid-state Lithium Batteries

Received 00th January 20xx,
Accepted 00th January 20xx

DOI: 10.1039/x0xx00000x

Yi Shi,[‡§a] Yang Chen,[‡ab] Yanliang Liang,[‡a] Justin Andrews,[c] Hui Dong,[a] Mengying Yuan,[d] Wenyue Ding,[e] Sarbajit Banerjee,[c] Haleh Ardebili,[d] Megan L. Robertson,[e] Xiaoli Cui,[b] and Yan Yao*[a]

Covalently networked polymers offer desirable non-crystallinity and mechanical strength for solid polymer electrolytes (SPEs), but the chemically active cross-links involved in their construction could deteriorate the compatibility with high-energy cathode materials that are electrophilic and/or in the charged state. Herein we reveal a strong dependence of cyclability of such cathodes on the reactivity of covalently networked SPEs and demonstrate a polymer design that renders these SPEs chemically inert. We designed and synthesized two hybrid networks, both with polyethylene oxide as the cation conduction component and polyhedral oligomeric silsesquioxane as branch point, but respectively uses the alkylamino and chemically inert triazole groups as cross-links. All-solid-state cells using the alkylamino-containing SPE underwent rapid degradation while cells using triazole SPEs showed stable cycling.

High-energy and safe lithium batteries for electrical energy storage and power supply have attracted tremendous interest because lithium metal has the highest theoretical capacity (3860 mAh g^{-1}) and lowest electrochemical potential (−3.04 V) among metal anodes.[1,2] However, metallic lithium dendrite growth and flammable liquid electrolytes and their side reaction with lithium metal compromise the safety of lithium batteries. Solid electrolytes may physically block lithium dendrites and avoid the flammability issues of liquid electrolytes, thereby lead to safe lithium batteries.[3-9] Various solid electrolytes that have been reported to date,[10-16] among which solid polymer electrolytes (SPEs)-based on polyethylene oxide (PEO) have received considerable interest owing to their strong lithium-ion solvating ability, easy processing, low density, and tunable structure.[17,18] SPEs based on unmodified PEO show low ion conductivity and mechanical strength which have limited their application for solid electrolytes. Several strategies have been developed to solve these problems, such as using PEO-based block/star/graft copolymers,[19-24] nanostructured polymers,[25-28] composite polymers,[29,30] networked polymers,[3,8,31,32] etc. In particular, covalently networked SPEs showed high ionic conductivity, great mechanical strength and excellent lithium dendrite growth resistance.[3,4,8] However, most cross-linked SPEs were prepared via polymerization aided by radical initiators or catalysts such as free radicals, which are highly reactive with lithium metal.[24,33-35] Recently, catalyst-free organic curing reactions such as epoxy-amino curing (EAC) reaction has been applied to prepare cross-linked SPEs.[4,8,36] However, the formed alkylamino groups are known to have low anodic stability.[37,38] While these SPEs appeared to be stable when paired with $LiFeO_4$ which is non-electrophilic when assembled into a cell

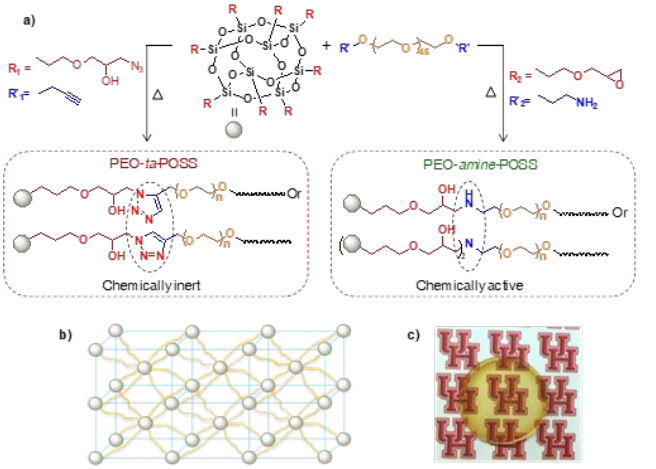

Figure 1 a) The synthesis route and chemical structure of PEO-POSS cross-linked SPEs, b) schematic structure of the network, c) photograph of a 200-μm-thick membrane of 4PEO-ta-POSS.

[a] *Department of Electrical and Computer Engineering and TcSUH, University of Houston, Houston, Texas 77204, United States. Email: yyao4@uh.edu*
[b] *Department of Materials Science, Fudan University, Shanghai 200433, China*
[c] *Department of Materials Science and Engineering, Texas A&M University, Texas 77843, United States*
[d] *Department of Mechanical Engineering, University of Houston, Houston, Texas 77204, United States*
[e] *Department of Chemical and Biomolecular Engineering, University of Houston, Houston, Texas 77204, United States*
[§] *Current address: School of Materials Science and Engineering, Sun Yat-Sen University, Guangzhou 510275, China*
† Electronic Supplementary Information (ESI) available: See DOI: 10.1039/x0xx00000x
‡ These authors contributed equally.

and requires a relatively low charging potential among commercial lithium cathode materials, we found that, as will be shown below, they have compatibility issues with several other categories of cathode materials, with which high-energy lithium batteries are being researched. It remains a challenge to develop SPEs that simultaneously provide high ionic conductivity, mechanical strength, and chemical inertness toward both lithium metal and high-voltage cathode materials.

Herein, we applied catalyst-free azide-alkyne cycloaddition (AAC) reaction to prepare chemically inert and covalently networked hybrid polymer electrolytes, PEO-*ta*-POSS (Fig. 1a), where PEO serves as the lithium-ion solvating component, the inorganic polyhedral oligomeric silsesquioxane (POSS) as branch point, and, most importantly, the oxidation-resistant triazole (*ta*) as the cross-link. For comparison, PEO-*amine*-POSS with alkylamino groups as the cross-link was also prepared. A series of cathode materials with varying properties were applied to investigate the electrochemical performance of the SPEs, including: poly(benzoquinonyl sulfide) (PBQS),[39] a representative of organic carbonyl compounds which are electrophilic and expected to be high-energy cathodes for lithium batteries;[40,41] ξ-V_2O_5, an high-capacity intercalation compound that has a high open-circuit voltage of 3.8 V vs Li^+/Li and could deliver higher energy than that of most commerical cathodes;[42] and $LiFePO_4$,[43] by far the most investigated cathode in SPE studies. We show that the chemical inertness of PEO-*ta*-POSS is critical for achieving high capacity and stable cycling.

The hybrid SPEs are easily constructed via catalyst-free organic curing reaction between functionalized POSS and PEO in the existence of LiTFSI ([EO]:[Li] = 16:1) in a one-pot process. The functionalized POSS and PEO as well as LiTFSI were dissolved in acetonitrile, and then the solution drop-casted in a PTFE mold. The thin membrane of cross-linked PEO-POSS SPEs were obtained after curing and thorough removal of solvent (Fig. 1c). The nPEO-*ta*-POSS's (n = 2, 4, and 6, n denotes the molar ratio of PEO to POSS) were synthesized from POSS-$(N_3)_8$ (Fig. 1, and Fig. S1 in Supporting Information) and PEO-dialkynyl (Fig. 1 and Fig. S2). As shown in Fig. S3a and b, the characteristic absorption of azido groups at 2111 cm^{-1} was absent when the molar ratio of [PEO]:[POSS] was 4:1 and 6:1, and the characteristic absorption of alkynyl groups at 2740 cm^{-1} disappeared when the molar ratio of [PEO]:[POSS] was 2:1 and 4:1, indicating complete AAC coupling reaction and formation of cross-linked network. The azido and alkynyl absorption band remained when the molar ratio of [PEO]:[POSS] was 2:1 and 6:1 due to an excess of POSS-$(N_3)_8$ and PEO-dialkynyl respectively. Meanwhile, the 4PEO-*amine*-POSS was prepared by EAC reaction and confirmed by FT-IR: after the reaction, the absorption of epoxy groups at 907 cm^{-1} disappeared, indicating complete reaction between epoxy and alkylamino groups and formation of crosslinked network (Fig. S4).

The phase behaviors of the hybrid SPEs were studied by differential scanning calorimetry (DSC). All the hybrid SPEs only show the glass transition and no melting points, indicating that the crystallization of PEO is completely suppressed (Fig. 2a). The amorphous phases were confirmed by the peak-less XRD patterns (Fig. 2b). The mechanical properties of the cross-linked SPEs were measured by dynamic mechanical analysis (DMA) in tensile mode (Fig. 2c and Table 1). All SPEs except 6PEO-*ta*-POSS show constant storage moduli (*E'*) above glass transition temperature and up to 130 °C. 6PEO-*ta*-POSS shows increased *E'* between 0 and 40 °C due

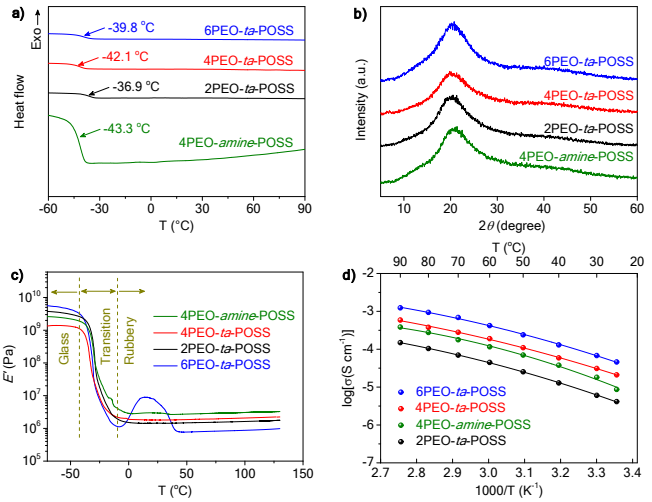

Figure 2 a) DSC curves, b) XRD patterns, c) storage modulus E', and d) ionic conductivity of PEO-POSS cross-linked polymer electrolytes.

to cold crystallization.[3] Such thermal stability contrasts with PEO-based electrolytes which soften/melt at >60 °C. The modulus of PEO-*ta*-POSS reaches a maximum of its highest at the [PEO]:[POSS] ratio of 4:1 when the azido and alkynyl groups are at equimolar amounts. Figure 2d shows the temperature-dependent ionic conductivity of cross-linked SPEs. At room temperature, the conductivity of PEO-*ta*-POSS SPEs are one to two orders of magnitude higher than that of PEO (~10^{-6} S cm^{-1}) and comparable to the best reported values (~10^{-4} S cm^{-1}) in crosslinked SPEs.[3,44-46] The ionic conductivity of PEO-*ta*-POSS SPEs increases from 1.5 × 10^{-4} (2PEO-*ta*-POSS) to 5.9 × 10^{-4} (4PEO-*ta*-POSS) to 1.2 × 10^{-3} S cm^{-1} (6PEO-*ta*-POSS) at 90 °C, which is attributed to the increasing PEO content. The ionic conductivity of 4PEO-*amine*-POSS 3.8 × 10^{-4} S cm^{-1} is close to that of 4PEO-*ta*-POSS. In this study, the ionic conduction mainly depends on the PEO segments, and the triazole groups mainly serve as the cross-link. Other stable functional groups may also serve as the cross-link, provided that they can be formed via reactions that have near-unity yield require under mild conditions. The ionic conductivities are further fitted using Vogel-Tammann-Fulcher (VTF) model (Fig. S5),[46] and the ionic transport activation energy is 8.4 kJ mol^{-1} (2PEO-*ta*-POSS), 8.2 kJ mol^{-1} (4PEO-*ta*-POSS), 7.8 kJ mol^{-1} (6PEO-*ta*-POSS), and 8.3 kJ mol^{-1} (4PEO-*amine*-POSS) (Table S1). This result agrees with a previous analysis that, within the same electrolyte class, a high ionic conductivity corresponds to a small activation energy.[44,46]

Table 1. Summary of PEO-POSS SPEs.

Sample [a]	Molar ratio (PEO:POSS)	PEO content (wt.%)	T_g (°C)	E'(MPa)	σ (S cm^{-1})			t (Li^+)
					30 °C	60 °C	90 °C	
2PEO-*ta*-POSS	2:1	71.6	-36.9	1.6	6.1E-6	4.5E-5	1.5E-4	0.17

4PEO-*ta*-POSS	4:1	83.5	-42.1	2.0	3.1E-5	1.9E-4	5.9E-4	0.30
6PEO-*ta*-POSS	6:1	88.4	-39.8	0.9	6.8E-5	4.2E-4	1.2E-3	0.20
4PEO-*amine*-POSS	4:1	85.9	-43.3	3.0	1.8E-5	1.1E-4	3.8E-4	0.11

[a] All sample had LiTFSI, [EO]:[Li$^+$] = 16:1

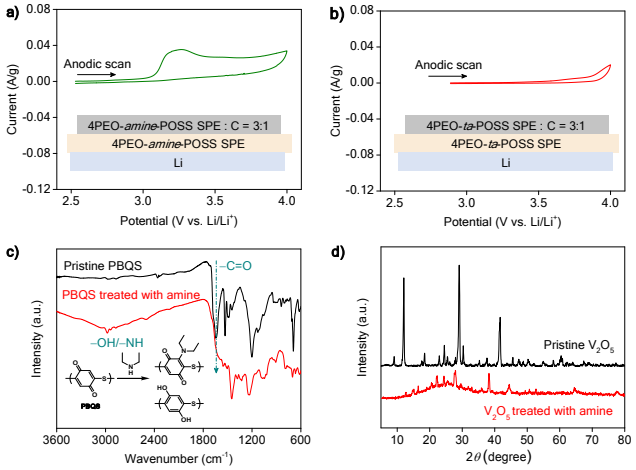

Figure 3 The electrochemical and chemical stability of PEO-POSS SPEs. CV curves of (a) Li/PEO-*amine*-POSS SPE/C and (b) Li/PEO-*ta*-POSS SPE/C cells at 0.2 mV s^{-1}. (c) The FT-IR spectra of PBQS before and after treatment with amine. (d) The XRD patterns of V_2O_5 before and after treatment with amine.

Li/PEO-POSS SPE/Li symmetric cells were assembled to evaluate Li/SPEs interfacial stability. Galvanostatic lithium plating and striping performance was recorded at 0.3 mA cm^{-2} with a specific capacity of 0.3 mAh cm^{-2} (Fig. S6). Compared to 2PEO-*ta*-POSS, 4PEO-*ta*-POSS and 6PEO-*ta*-POSS showed better stability and lower voltage polarization with initial area specific resistance (ASR) of 312 and 318 Ω cm^2, respectively, which were benefited from the higher ionic conductivities. The voltage profiles agree with the Li$^+$ transference number: a higher Li$^+$ transference number (Table 1 and S2, Fig. S7) corresponds to a flatter voltage plateau.[47,48] In 4PEO-*amine*-POSS, the amino group can coordinate with Li-ions and trap them as defect sites, which interaction may have led to the lower Li-ion transference number. The Li-ion transference number of 4PEO-*ta*-POSS is the largest among the xPEO-*ta*-POSS's because there are least unreacted functional groups (e.g. alkynyl and azido groups) which may coordinate with Li-ions. Even higher transference number may be possible if less coordinating polymers such as cyano-containing ones are used in place of PEO.

The electrochemical stability of PEO-*ta*-POSS and PEO-*amine*-POSS SPEs was evaluated using Li/PEO-POSS SPE/C cells where the cathode is composed of a mixture of the SPEs and conductive carbon (Fig. 3a). Such a composite electrode is a close approximation of a battery cathode where the SPE and conductive carbon are thoroughly mixed and have a large contact area. Such a composite electrode is a close approximation of a battery cathode where the SPE and conductive carbon are thoroughly mixed and have a large contact area. The electrode can therefore more precisely measure the electrochemical stability window of SPEs than a traditional planar electrode which has a limited contact area.[49,50] A broad irreversible anodic peak appears above 3.0 V for 4PEO-*amine*-POSS, indicating instabilities of the polymer at high potentials. In contrast, anodic current was only observed above 3.8 V for 4PEO-*ta*-POSS. The chemical stability of the SPEs was probed by directly treating cathode materials with diethylamine, which resembles the dialkylamino group in 4PEO-*amine*-POSS. A suspension of PBQS in a solution of diethylamine in tetrahydrofuran was stirred at room temperature for 12 h. The C=O absorption of PBQS at 1647 cm^{-1} almost disappeared after the reaction, and a broad absorption at 3129 cm^{-1} corresponding to –OH appeared, indicating that the majority of quinone units had been converted into hydroquinone (Fig. 3b). A similar model reaction between V_2O_5 and diethylamine led to a complete conversion of V_2O_5 into an unidentified compound, as detected by XRD pattern (Fig. 3c). These undesired reactions become more severe at the cell testing temperatures (60–90 °C).

The cell performance of PEO-*ta*-POSS and PEO-*amine*-POSS SPEs were investigated in lithium cells at 90 °C. The Li/4PEO-*ta*-POSS SPE/PBQS cell showed a stable capacity of 153 mAh g^{-1} at 0.1C (Fig. 4a). while the capacity of Li/4PEO-*amine*-POSS SPE/PBQS decreased from 62 to 50 mAh g^{-1} in the first 3 cycles with large irreversible charge capacities (Fig. 4b). After 50 cycles, the stable capacity of Li/4PEO-*amine*-POSS SPE/PBQS was only 35 mAh g^{-1}, a quarter of that of Li/4PEO-*ta*-POSS SPE/PBQS (Fig. 4c). Similar stability difference was found for Li/PEO-POSS SPE/V_2O_5 cells. Li/4PEO-*ta*-POSS SPE/V_2O_5 cell showed a reversible specific capacity of 245 mAh g^{-1} and maintained 223 mAh g^{-1} after 50 cycles, corresponding to a 91% capacity retention (Fig. 4d, f). Li/4PEO-*amine*-POSS SPE/V_2O_5 cell showed a low coulombic efficiency at the first cycle and lost 95% of its initial capacity after 10 cycles (Fig. 4e, f). The inferiority of the SPEs with alkylamino cross-link was not seen in the literature probably because of the cathode material used in previous covalently networked SPE studies, which was almost always $LiFePO_4$. The performance difference between the two SPEs was not as drastic with a $LiFePO_4$ cathode: while a Li/4PEO-*ta*-POSS SPE/$LiFePO_4$ cell showed a higher and more stable specific capacity

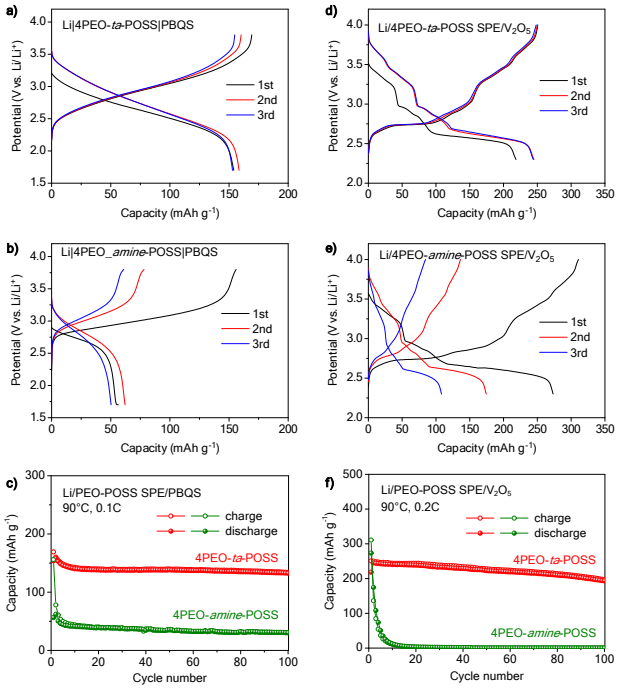

Figure 4 The electrochemical performance of Li/PEO-POSS SPE/PBQS (a–c) and Li/PEO-POSS SPE/V_2O_5 cells (d–f) at 90 °C. (a, d) The voltage profiles of first three cycles using 4PEO-*ta*-POSS SPE. (b, e) The voltage profiles of first three cycles using 4PEO-*amine*-POSS SPE. (c, f) Comparison of the cycling performance of each cathode material in the two SPEs.

of 156 mAh g^{-1} (Fig. S8a), a Li/4PEO-*amine*-POSS SPE/$LiFePO_4$ cell held its own with a usable though less stable specific capacity of ~120 mAh g^{-1} (Fig. S8b).

We have checked the morphology of Li/SPE/PBQS cells after 300 cycles. Fig. S9 shows the cross-sectional SEM images of the cells using (a, c) 4PEO-*amino*-POSS SPE and (b, d) 4PEO-*ta*-POSS SPE, respectively. In Fig. S9(a), interdiffusion between cathode materials and 4PEO-*amino*-POSS polymer electrolytes was observed as the result of the chemical reactivity between PBQS and 4PEO-*amino*-POSS SPE, leading to the absence of a cathode-SPE interface. In contrast, a clear cathode-SPE interface between PBQS and proposed 4PEO-*ta*-POSS SPE as can be observed in Fig. S9(b), indicating the chemical inertness. A uniform lithium deposition, as seen in Fig. S9(c, d), indicates that both 4PEO-*amino*-POSS and 4PEO-*ta*-POSS SPE can suppress the growth of lithium dendrites. Note that some lithium was plated on the surface of 4PEO-*ta*-POSS SPE at the interface, which may result in an increase of Li-SPE interfacial resistance.

The AC impedance of Li/4PEO-*amino*-POSS SPE/PBQS and Li/4PEO-*ta*-POSS SPE/PBQS cell after 300 cycles were also measured over a frequency range of 10^6-0.1 Hz with a 7-mV amplitude. The plots were fitted by the inserted equivalent circuit models by ZView software, and corresponding parameters were listed in Table S3 and S4. R_e stands for bulk resistance of the polymer electrolyte; R_1 and CPE_1 represent the charge transfer resistance and interfacial capacitance of Li-SPE interface; R_2 and CPE_2 represent the charge transfer resistance and interfacial capacitance of cathode-SPE interface; *W* stands for Warburg resistance. Fig. S10(c, d) show the Nyquist plots of cycled Li/4PEO-*amino*-POSS SPE/PBQS and Li/4PEO-*ta*-POSS SPE/PBQS cell. Upon cycling, the polymers and LiTFSI decompose continuously on the lithium surface[36,51], leading to an enlargement of R_e and R_1 compared with those of the fresh cells. The cathode-SPE interfacial resistance (R_2) of Li/4PEO-*amino*-POSS SPE/PBQS cell was about one eighth that of Li/4PEO-*ta*-POSS SPE/PBQS cell. The chemical reaction between PBQS and 4PEO-amino-POSS SPE leading to a well-contacted cathode-SPE interface, and thus a much smaller interfacial resistance.

The examples above show that the (electro)chemical inertness of SPEs' is a prerequisite for enabling high-energy cathode materials in a covalently networked SPE-based solid-state cell. The use of triazole as an unreactive cross-link for PEO-POSS eliminates the anodic instability and chemical reactivity found for alkylamino and alkyl sulfide groups typically used for constructing such polymers. The fact that the three cathode materials all work satisfactorily in the electrolyte indicates the universality of the strategy for high-performance SPE design.

Conclusions

In summary, we have developed covalently networked polymer electrolytes cross-linked by triazole groups via a facile catalyst-free AAC reaction for all-solid-state lithium batteries. The polymer design avoids residual reactive agents and cross-link groups in the electrolyte, thus leading to (electro)chemical inertness rarely found for covalently networked SPEs. The triazole-based PEO-*ta*-POSS SPEs expand the electrochemical stability window by 800 mV compared with a structurally similar SPE cross-linked by alkylamino groups. Multiple categories of potentially high-energy cathode materials were found to charge and discharge stably in the PEO-*ta*-POSS SPEs, whereas they all undergo rapid capacity fade in the alkylamino-based SPE. Control cells and reactions indicate strong dependence of cell performance on the reactivity of the SPEs. Our approach provides new design space for developing polymer electrolytes that simultaneously offer the mechanical strength, ionic conductivity, and, most importantly, chemical stability for SPE-based solid state batteries.

Acknowledgements

We acknowledge the funding support from the U.S. Department of Energy's Office of Energy Efficiency and Renewable Energy (EERE), as part of the Battery 500 Consortium (# DE-EE0008234). Y.C. thanks the funding from China Scholarship Council.

Conflicts of interest

There are no conflicts to declare.

Notes and references

1. W. Xu, J. Wang, F. Ding, X. Chen, E. Nasybulin, Y. Zhang and J.-G. Zhang, *Energy Environ. Sci.*, 2014, **7**, 513-537.
2. Y. Lu, Z. Tu and L. A. Archer, *Nat. Mater.*, 2014, **13**, 961.
3. R. Khurana, J. L. Schaefer, L. A. Archer and G. W. Coates, *J. Am. Chem. Soc.*, 2014, **136**, 7395-7402.
4. Q. Lu, Y. B. He, Q. Yu, B. Li, Y. V. Kaneti, Y. Yao, F. Kang and Q. H. Yang, *Adv. Mater.*, 2017, **29**, 1604460.
5. X.-X. Zeng, Y.-X. Yin, N.-W. Li, W.-C. Du, Y.-G. Guo and L.-J. Wan, *J. Am. Chem. Soc.*, 2016, **138**, 15825-15828.
6. A. Sharafi, E. Kazyak, A. L. Davis, S. Yu, T. Thompson, D. J. Siegel, N. P. Dasgupta and J. Sakamoto, *Chem. Mater.*, 2017, **29**, 7961-7968.
7. F. Han, J. Yue, X. Zhu and C. Wang, *Adv. Energy Mater.*, 2018, **8**, 1703644.
8. Q. Pan, D. M. Smith, H. Qi, S. Wang and C. Y. Li, *Adv. Mater.*, 2015, **27**, 5995-6001.
9. P. Zhu, C. Yan, J. Zhu, J. Zang, Y. Li, H. Jia, X. Dong, Z. Du, C. Zhang, N. Wu, M. Dirican, X. Zhang, *Energy Storage Mater.,* **2019**, *17*, 220-225.
10. A. Varzi, R. Raccichini, S. Passerini and B. Scrosati, *J. Mater. Chem. A*, 2016, **4**, 17251-17259.
11. H. Zhang, C. Li, M. Piszcz, E. Coya, T. Rojo, L. M. Rodriguez-Martinez, M. Armand and Z. Zhou, *Chem. Soc. Rev.*, 2017, **46**, 797-815.
12. Z. Zhu, M. Hong, D. Guo, J. Shi, Z. Tao and J. Chen, *J. Am. Chem. Soc.*, 2014, **136**, 16461-16464.
13. J. Janek and W. G. Zeier, *Nat. Energy*, 2016, **1**, 16141.
14. J. Zhang, X. Li, Y. Li, H. Wang, C. Ma, Y. Wang, S. Hu, W. Wei, *Front. Chem.,* **2018**, *6*, 168.
15. Q. Wang, H. Zhang, Z. Cui, Q. Zhou, X. Shangguan, S. Tian, X. Zhou, G. Cui, *Energy Storage Mater.,* **2019**, doi.org/10.1016/j.ensm.2019.04.016
16. J. Zhang, J. Zhao, L. Yue, Q. Wang, J. Chai, Z. Liu, X. Zhou, H. Li, Y. Guo, G. Cui, L. Chen, *Adv. Energy Mater.* **2015**, 5, 1501082.

17. M. A. Morris, H. An, J. L. Lutkenhaus and T. H. Epps, *ACS Energy Lett.*, 2017, **2**, 1919-1936.
18. Z. Xue, D. He and X. Xie, *J. Mater. Chem. A*, 2015, **3**, 19218-19253.
19. P. R. Chinnam, S. L. Wunder, *Chem. Mater.,* 2011, 23, 5111-5121.
20. Y. Chen, Y. Shi, Y. Liang, H. Dong, F. Hao, A. Wang, Y. Zhu, X. Cui, Y. Yao, *ACS Applied Energy Mater.* **2019**, 2, 1608-1615.
21. C. M. Bates, A. B. Chang, N. Momčilović, S. C. Jones and R. H. Grubbs, *Macromolecules*, 2015, **48**, 4967-4973.
22. R. Bouchet, S. Maria, R. Meziane, A. Aboulaich, L. Lienafa, J.-P. Bonnet, T. N. T. Phan, D. Bertin, D. Gigmes, D. Devaux, R. Denoyel and M. Armand, *Nat. Mater.*, 2013, **12**, 452.
23. R. Bouchet, T. N. T. Phan, E. Beaudoin, D. Devaux, P. Davidson, D. Bertin and R. Denoyel, *Macromolecules*, 2014, **47**, 2659-2665.
24. J. Ping, H. Pan, P. P. Hou, M.-Y. Zhang, X. Wang, C. Wang, J. Chen, D. Wu, Z. Shen and X.-H. Fan, *ACS Appl. Mater. Interfaces*, 2017, **9**, 6130-6137.
25. G. Yang, C. Chanthad, H. Oh, I. A. Ayhan and Q. Wang, *J. Mater. Chem. A*, 2017, **5**, 18012-18019.
26. M. W. Schulze, L. D. McIntosh, M. A. Hillmyer and T. P. Lodge, *Nano Lett.*, 2014, **14**, 122-126.
27. L. D. McIntosh, M. W. Schulze, M. T. Irwin, M. A. Hillmyer and T. P. Lodge, *Macromolecules*, 2015, **48**, 1418-1428.
28. E. Glynos, L. Papoutsakis, W. Pan, E. P. Giannelis, A. D. Nega, E. Mygiakis, G. Sakellariou and S. H. Anastasiadis, *Macromolecules*, 2017, **50**, 4699-4706.
29. H. Zhang, S. Kulkarni and S. L. Wunder, *J. Electrochem. Soc.*, 2006, **153**, A239-A248.
30. J. Zhang, X. Zang, H. Wen, T. Dong, J. Chai, Y. Li, B. Chen, J. Zhao, S. Dong, J. Ma, L. Yue, Z. Liu, X. Guo, G. Cui, L. Chen, *J. Mater. Chem. A*, **2017**, *5*, 4940-4948.
31. J. Hu, W. Wang, H. Peng, M. Guo, Y. Feng, Z. Xue, Y. Ye and X. Xie, *Macromolecules*, 2017, **50**, 1970-1980.
32. Q. Zheng, L. Ma, R. Khurana, L. A. Archer and G. W. Coates, *Chem. Sci.*, 2016, **7**, 6832-6838.
33. J.-A. Choi, Y. Kang, H. Shim, D. W. Kim, H.-K. Song and D.-W. Kim, *J. Power Sources*, 2009, **189**, 809-813.
34. K. M. Kim, B. Z. Poliquit, Y.-G. Lee, J. Won, J. M. Ko and W. I. Cho, *Electrochimica Acta*, 2014, **120**, 159-166.
35. H. Wu, Y. Cao, H. Su and C. Wang, *Angew. Chem. Int. Ed.*, 2018, **57**, 1361-1365.
36. Q. Pan, D. Barbash, D. M. Smith, H. Qi, S. E. Gleeson and C. Y. Li, *Adv. Energy Mater.*, 2017, **7**, 1701231.
37. R. L. Hand and R. F. Nelson, *J. Am. Chem. Soc.*, 1974, **96**, 850-860.
38. Y. Shi, D. J. Noelle, M. Wang, A. V. Le, H. Yoon, M. Zhang, Y. S. Meng and Y. Qiao, *ACS Appl. Mater. Interfaces*, 2016, **8**, 30956-30963.
39. Z. Song, Y. Qian, T. Zhang, M. Otani and H. Zhou, *Adv. Sci.*, 2015, **2**, 1500124.
40. Y. Liang, Y. Jing, S. Gheytani, K.-Y. Lee, P. Liu, A. Facchetti and Y. Yao, *Nat. Mater.*, 2017, **16**, 841.
41. Y. Liang and Y. Yao, *Joule*, 2018, **2**, 1690-1706.
42. G. A. Horrocks, A. Parija, L. R. De Jesus, L. Wangoh, S. Sallis, Y. Luo, J. L. Andrews, J. Jude, C. Jaye, D. A. Fischer, D. Prendergast, L. F. J. Piper and S. Banerjee, *Chem. Mater.*, 2017, **29**, 10386-10397.
43. F. Croce, S. Sacchetti and B. Scrosati, *J. Power Sources*, 2006, **162**, 685-689.
44. S. Liu, H. Wang, N. Imanishi, T. Zhang, A. Hirano, Y. Takeda, O. Yamamoto and J. Yang, *J. Power Sources*, 2011, **196**, 7681-7686.
45. C. N. Walker, C. Versek, M. Touminen and G. N. Tew, *ACS Macro Letters*, 2012, **1**, 737-741.
46. K. M. Diederichsen, H. G. Buss and B. D. McCloskey, *Macromolecules*, 2017, **50**, 3831-3840.
47. D. Lin, P. Y. Yuen, Y. Liu, W. Liu, N. Liu, R. H. Dauskardt and Y. Cui, *Adv. Mater.*, 2018, **30**, 1802661.
48. J. Evans, C. A. Vincent and P. G. Bruce, *Polymer*, 1987, **28**, 2324-2328.
49. J. Trevey, Y. S. Jung and S.-H. Lee, *ECS Transactions*, 2009, **16**, 181-187.
50. Y. Tian, T. Shi, W. D. Richards, J. Li, J. C. Kim, S.-H. Bo and G. Ceder, *Energy Environ. Sci.*, 2017, **10**, 1150-1166.
51. W. Zhou, H. Gao, J. B. Goodenough, *Adv. Energy Mater.* **2016**, *6*, 1501802.

Entry for the Table of Contents

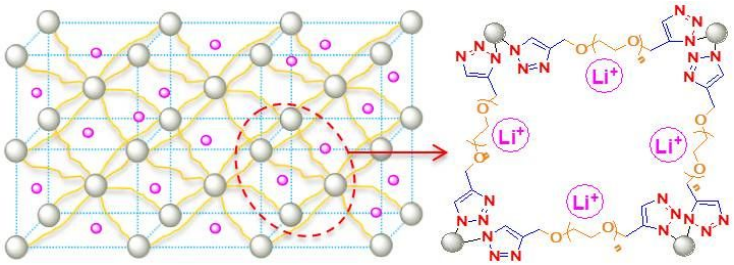

Chemically inert covalently networked solid polymer electrolyte with triazole groups as crosslinks was developed for all-solid-state lithium batteries.